E-9 FRACTURE MECHANICS AND RADIATION EMBRITTLEMENT

A. M. Sullivan[1]

ABSTRACT

Fracture tests were conducted on two irradiated pressure vessel steels. The stress intensity factor under plane strain, K_{Ic}, was calculated using the strain hardening coefficient, n, and the process zone size, d_T. Values obtained for K_{Ic} verify that irradiation seriously embrittles structural steels. Results of this investigation also reinforced the previously observed fact that strain at maximum load, while an indication of instability is not an ideal indicator of the fracture event. More appropriately, some value related to total elongation should be chosen. Practical considerations of the effect of radiation on both temperature and rate dependency of fracture toughness are discussed.

[1] Metallurgist, Mechanics Division, U.S. Naval Research Laboratory

NOMENCLATURE

a	Initial half crack length
b	Initial crack depth
d	Process zone dimension
d_T	Process zone dimension at instability
n	Strain hardening coefficient
r	Plastic zone dimension
r_Y	Plastic zone dimension at instability
B	Specimen thickness
C_p	Heat capacity
E	Young's elastic modulus
K	Stress intensity factor
K_c	Critical stress intensity factor under conditions of plane stress
K_{Ic}	Critical stress intensity factor under conditions of plane strain
$\dot{K}$	Stress intensity rate
M	Material constant
Q	(Subscript) adiabatic
T	(Subscript) isothermal
T	Temperature
V	Volume
W	Specimen width
$\bar{\delta}_c$	True strain in compression
ε	Strain
ε_c	Strain in compression
ε_{max}	Strain at maximum load

NOMENCLATURE (CONT'D)

ε_y	Normal strain in y-direction
$\dot{\varepsilon}$	Strain rate
ρ	Density
σ	Gross stress load/unnotched area
σ_f	Flow stress
σ_N	Net stress load/notched area
σ_y	Normal stress in y-direction
σ_{YS}	Yield stress
σ_{UYS}	Upper yield stress
θ	Tangent modulus ($d\sigma/d\varepsilon$)
cal.	Calorie (gram)
NDT	Nil Ductility Temperature
Wt	Weight

I. INTRODUCTION

The complexity of the undesired separations usually referred to as "brittle fracture" have generated an extensive literature representing diverse experimental philosophies. From the point of view of practicality, the concepts of linear elastic fracture mechanics have been explored and applied by Irwin and co-workers (1,2,3) to provide a rational basis for quantitative estimates of fracture toughness.

Briefly, fracture mechanics is a generalization of the Griffith energy balance relationship (4) and assumes that at the tip of a crack in any structure the distribution of stress normal to the crack, σ_y, can be described by the equation

$$\sigma_y = \frac{K}{\sqrt{2\pi r}} \qquad (1)$$

where K is a function of loads, crack size, and shape factors which can be known through theoretical or experimental analysis. Placing σ_y equal to the uniaxial tensile yield strength σ_{YS} provides a special length factor r_Y given by

$$r_Y = \frac{1}{2\pi}\left(\frac{K}{\sigma_{YS}}\right)^2 \qquad (2)$$

In linear elastic fracture analysis r_Y is customarily added to the crack size as a plasticity adjustment. As long as all crack-like flaws are less than 2 r_Y in size, a component can be expected to support a stress nearly as large as σ_{YS} prior to fracture. In general, the relationship between the fracture stress and the size of the starting crack is provided by measurements of the critical stress factor values K_c (K_{Ic} for plane strain) necessary for crack propagation.

In high strength brittle materials, where the plastic zone size is relatively small, both K_c and K_{Ic} can be determined accurately on specimens of convenient laboratory size. However, with tougher materials of lower strength, the problem of containment of the plastic zone within an elastic constraint becomes increasingly difficult. The body of experimental data examined using values of K_c showed clearly that this plane stress intensity factor was sensitive to geometrical considerations, namely, varying with specimen thickness and, at high stress levels, with specimen width. Although an analytic correction factor was developed to adjust for this effect, in general it has been found more practical to concentrate attention on K_{Ic}, the plane strain factor, which is less sensitive to geometry. However, it must still be recognized that when the nominal stress, σ_N, exceeds the yield stress σ_{YS} no true analysis is possible, since general yield precludes application of equations based on elastic conditions.

[1] Metallurgist, Mechanics Division, U. S. Naval Research Laboratory

There is a limiting minimum size for test specimens below which valid K_{Ic} measurements are not possible - and this limiting size is both material and yield stress dependent. Furthermore, for some materials, this minimum size will be impractically large - either for the material available or the testing machine capacity.

Establishment of some correlation factor between either yield or flow properties and K_{Ic} would enable calculations of stress intensity in situations where direct measurement is impossible. One such correlation with the upper yield strength, σ_{UYS}, is discussed by Krafft and Sullivan (5) where

$$K_{Ic} = M\,\sigma_{UYS}^{-1.5} \qquad (3)$$

(with M a material variant experimentally determined). Although this relationship appeared satisfactory for steels of low strength level, attempts to apply the relationship to metals of very high yield strength were unsuccessful.

A new approach by Krafft (6) considered strain hardening in relation to the strain field at the crack tip. As an analysis convention it was assumed that the strain ϵ at a distance d close to the crack tip is given by an equation similar in form to equation (1).

$$\epsilon_y = \frac{K/E}{\sqrt{2\pi d}} \qquad (4)$$

Now at some value of ϵ, tensile instability will occur and this value of ϵ can be equated to the strain at maximum load (tensile instability) to which is assigned the value of the strain hardening exponent n. Thus,

$$n = K_{Ic}/E/\sqrt{2\pi d_T} \qquad (5)$$

Equation (5) provides a new length factor d_T, much smaller than r_Y, and may be regarded as defining the size of a process zone within which strains have reached a maximum value for uniform flow. At larger strains instability (necking and fracture) ensues.

The basic idea is to use direct measurements of K_{Ic} at low temperature and high strain rate to find d_T. Equation (5) can then be used to estimate K_{Ic} for temperatures and strain rates such that the size of the plastic zone renders direct measurement impractical.

Temperature is easily known from operating conditions but strain rate or crack speed must be estimated from an analysis which takes into account the intensifying effect of the crack on the strain at instability.

Using equation (4) for this purpose we find

$$\frac{K_{Ic}/E}{n} = \frac{\dot{K}_{Ic}/E}{\dot{\epsilon}} = \sqrt{2\pi d_T} \qquad (6)$$

where $\dot{K}$ and $\dot{\epsilon}$ are the derivatives of K and ϵ with respect to time.

Since the process zone d_T appears constant over the ranges of temperature and rate studied, equation (5) or (6) can be utilized to evaluate K_{Ic} at temperatures and loading rates where direct measurement is virtually impossible. This indirect approach is especially valuable in studies of the effects of irradiation, where limited reactor space for the irradiation of research samples makes mandatory the determination of the stress intensity factor on a miniaturized scale.

The investigations detailed here are on two low strength pressure vessel steels, in both the as received and irradiated condition. The stress intensity parameter K_{Ic} is measured directly on small center notched sheet specimens at temperatures and loading rates when this is feasible. Establishment of the correlation factor then permits calculated estimates of K_{Ic} at extended ranges of operating condition.

II. MATERIALS AND SPECIMENS

The two steels discussed here are an A350LF3 (sister forging to that used in the pressure vessel of the PM2A Army Reactor) extensively studied by Steele and co-workers (7); and a commercial A212B. Compositions are in Table I. The reactor package used, Figure 1, had four compartments; Charpy specimens and plugs in the outer ones and center notched sheet tensile specimens in the center. Though no flux monitors were placed in the center packages, hardness measurements for all specimens of the same steel were identical. The package was irradiated in the Oak Ridge Research Reactor. After one month in core position D-1, the package was rotated and up-ended to equalize the dosage; it was then returned to the reactor, but to position D-2, for a second month.

Monitors showed that the following temperatures were reached, Table II. Unfortunately, some leakage occurred in the outer package (Charpy and plugs) for the A350LF3. The total integrated neutron exposure as determined from flux monitors was $1.33\text{-}1.36 \times 10^{20}$ n/cm^2.

Three different specimens were incorporated in the package: standard Charpy V-notch beams; plugs (rectangular compression specimens) .394 in. square (1 cm) and .72 in. (1.8 cm) high; center notched sheet specimens 6.5 in. (16.5 cm) long, 1.7 in. (4.31 cm) wide, and 0.1 in. (.25 cm) thick containing a center crack (2a) .765 in. (1.94 cm) in length prepared by an electric discharge method (Elox). The radius of the crack tip was further reduced by honing with a sharpened blade, but was not fatigued since at the time of specimen preparation a satisfactory method for this procedure had not yet been developed.

III. TESTING PROCEDURES AND DATA REDUCTION

All tests were performed using the Dynamic Universal Loader Model I, developed at NRL by Krafft and Hahn. This apparatus has been discussed in other publications (8), but briefly, it is a hydraulically stiffened machine loaded with bottled nitrogen gas and fitted with a double-acting valve which permits operation in both tension and compression. The range of head speeds covered is about five orders of magnitude

(say $\dot{\epsilon}$ 10^{-3} to 5×10^{1}) and a maximum load of 40 kips is developed.

First, according to customary practice, compression tests are run at a series of temperatures covering the Charpy range and at four or five different head speeds.

Load-displacement measurements are recorded on a Tektronix No. 536 X-Y Oscilloscope. A four-gage Wheatstone bridge circuit (A-7, SR-4, 120 Ω, GF 2.0) arranged on a weigh bar in train with the specimen provides load information, while a set of cantilever beams instrumented by A-5, SR-4 gages attached to the head and driven by the load anvil through a grooved collar give displacements. Timing modulations, provided by a standard time-mark generator, enable head speed, strain-rate, etc. to be accurately determined.

Flow stress at 3 percent strain is plotted in Figure 2a and b. Data are derived from records similar to those of Figure (2c), yield stress, flow stress at 3 percent strain and θ, the tangent modulus at 3 percent strain, being read together with the strain rate. The adiabatic strain hardening coefficient, n_Q, is then computed from the relationship

$$n_Q = \epsilon \left(\frac{\theta}{\sigma_f} - 1 \right) \tag{7}$$

At present in this experimental set up, it is not possible to monitor directly changes in diameter with increased load. However, utilizing the relationship established (assuming constant volume) one may compute true stress and true strain from the data available:

$$\bar{\sigma}_c = \sigma_c (1 - \epsilon_c) \tag{8}$$

$$\bar{\delta}_c = \epsilon_c \frac{1}{(1 - \epsilon_c)} \tag{9}$$

When these values are plotted on log-log paper, and the slope of the curve is measured, n_Q is found to agree closely, (within about 2%) of values computed according to equation (7). Total strain in these specimens is rarely over 12% so end effects and barrelling are minimized. (Later work has utilized molybdenum disulfied in grooves scribed on the ends to further eliminate frictional effects).

However, since the relationship established by Krafft, equation (6) correlates K_{Ic} to the isothermal value of the strain hardening coefficient, this value n_T is computed from the following equation of state relationship:

$$n_T = \frac{\epsilon}{\sigma_{f_T}} \left\{ \theta_Q - \left(\frac{\partial \sigma}{\partial T} \right) \left(\frac{dT}{d\epsilon} \right) \right\} - \epsilon \tag{10}$$

where ϵ is again set at 3% where flow stress, σ_f, and tangent modulus, θ, are measured.

The flow stress-temperature sensitivity is determined by replotting the flow stress (selected at regular intervals of strain rate) against temperature. The slopes of curves fitted through these points give a family of curves ($\partial\sigma/\partial T$) at appropriate temperatures. $dT/d\epsilon$ is a function of the external work and heat capacity such that

$$\Delta T = \frac{cal}{C_p W_t} = \frac{cal}{C_p \rho V} = \frac{\sigma V d\epsilon}{C_p \rho V} \qquad (11)$$

and

$$\frac{dT}{d\epsilon} = \frac{\sigma}{C_p \rho} = \frac{\sigma_{f_Q}}{C_p} \times (2.10 \times 10^{-4}) \quad \text{CGS Units}$$

$$= \frac{\sigma_{f_Q}}{C_p} \times (3.78 \times 10^{-4}) \quad \text{English units} \qquad (12)$$

using appropriate values of C_p as it changes with temperature. Values of ΔT are computed for arbitrary levels of σ_f and plotted against temperatures so that the actual test temperature can be used for computation, and the term between brackets becomes θ_T ($d\sigma_T/\sigma\ \epsilon$); isothermal flow stress can then be computed as

$$\sigma_{f_T} = \sigma_{YS} + \theta_T d\epsilon \qquad (13)$$

Fracture specimens, center notched sheet in this case, are pulled in tension over a range of head speeds and at suitable temperatures for valid results. The appropriate equation for this specimen as discussed by Irwin (9, 10) and the special ASTM committee (11) is

$$K_{Ic} = \sigma\sqrt{W \tan \frac{\pi a}{W}} \qquad (14)$$

Data are plotted on log-log paper as

a. n vs $\dot{\epsilon}$

b. K_{Ic}/E vs $\dot{K}_{Ic}/E$

and superposition along a constant ratio match line gives the correlation factor, equation (6).

Utilizing this factor, all strain hardening values can be converted into K_{Ic} values in the temperature and rate range where valid fracture tests are impossible (general yielding) or impractical (specimen size, etc.) and data are shown in Figure 3.

IV. RESULTS

K_{Ic} and yield stress value plotted in Figure (4) against temperature indicate that a nice discrimination is readily obtained for the subject

steels in both the as-received and irradiated condition. Values have been chosen at a rate compatible with that of the Charpy test ($\dot{K} = 10^8$) (5) and are isothermal. In an earlier paper discussing the correlation factor relationship (12) adiabatic values were reported as representing a minimum level. Now, however, from tests performed at NRL on the double cantilever beam specimen which directly measures "arrest" values, it appears that the higher isothermal values are more realistic.

The yield stress values which remain high over the temperature range surveyed are coupled with extremely low K_{Ic} values. The transposition of the curves for the irradiated steels is reflected in the more familiar Charpy data for the same materials Figure (5). Changes in the parameters are indicated in Table III. These values are quite compatible with those previously reported for the same steel (A350LF3) by the NRL Metallurgy Division (7).

The process zone size, d_T, which still appears insensitive to temperature and strain rate, now shows an apparent enlargement, Table IV.

Conversely, it is observed that the measurement capacity of the specimen is diminshed. This value is defined by relating the specimen thickness to the plastic zone size, $r_Y = \frac{1}{2\pi}\left(\frac{K_{Ic}}{\sigma_{YS}}\right)^2$. At low temperatures when valid K_{Ic} determinations are possible on the small center notched sheet specimens at a selected Charpy temperature (C_V 30 ft-lbs) this ration B/r_Y is seen altered in Table V.

Of even more immediate interest, however, are the values of $K_{Ic}(T)$ at temperatures corresponding to NDT of the drop weight test. For the control material, increasing with lowered NDT, they are shown to vary with yield strength providing an independent verification of the correlation required by the Pellini fracture analysis diagram.

However useful this relationship may be for control materials, it is no longer exhibited by these steels in the irradiated condition. Now, although K_{Ic} still varies with yield stress, it does so inversely and the slope of this curve differs with material, Figure (6).

V. POSTULATED FLAW SIZE

The practical nature of fracture mechanics parameters arises from the fact that design criteria are implicit in the definitions: operating stress level and/or critical crack size.

In this study, the steels chosen are typical of those used in vessels enclosing the pressurized coolant of a reactor heat source. The stress levels, allowed by design and operation, are established relative to the yield strength of the material prior to irradiation hardening.

In such a situation, a suitable expression for fracture toughness assuming a part-through crack is provided by the equation

$$K_{Ic} = \frac{\sigma\sqrt{1.2\pi b}}{E_k^2 - 0.212\left(\frac{\sigma}{\sigma_{YS}}\right)^2}^{1/2}$$

where E_k is a commonly tabulated elliptic integral.

$$E_k = \int_0^{\pi/2} \sqrt{1 - k^2 \sin^2 \varphi}\, d\varphi$$

$$k^2 = 1 - (b/a)^2$$

Irwin's discussions of this expression may be found in reference (13). Calculated flaw depths b are plotted against temperature in Figure 7 for a postulated circular flaw shape; other shapes will give crack depths less than these and the equation is valid only for cracks less than one half the wall thickness.

A comparison of static and dynamic loading is provided since, once the crack becomes unstable through static loading, crack speed acceleration will cause the dynamic values to apply.

Irradiation markedly reduces the flaw sizes which can be tolerated, although less difference is noted between static and dynamic values.

VI. SPECULATIONS CONCERNING THE PROCESS ZONE

Although obviously a convenient correlation concept, to be really meaningful, the physical nature of the process zone must also be considered.

The model proposed by Krafft appears to be that ligaments of a size proportional to d_T are progressively ruptured as the crack advances to separate the fracturing surfaces. He suggests that these ligaments fracture as in typical cup-cone tensile specimens and that this process is reflected in the "dimple" structure seen on electron micrographs of "ductile fracture" surfaces.

It does appear from examination and measurement of these dimples that they:

1. Vary with material
2. Vary with impurity content
3. Appear "seeded by inclusions"
4. Vary in a manner that appears to be a proportionate function of d_T
5. Are unchanged with test temperature or loading rate.

However, the dimples are extremely non-uniform in size and earlier work, Edwards (14), indicated that they do decrease in depth at lowered temperature. Furthermore, they cannot be distinguished on the fracture surfaces (cleavage) of steels at the low temperature where the tests are made to establish the ratio which fixes the (constant) value of d_T used; nor are they conspicuously visible on fracture surfaces produced by fatigue methods.

In view of the more sophisticated analyses of the deformation processes available in the now well-developed models of dislocation behavior, it seems worthwhile to consider this more "atomistic" view. Development of techniques for transmission electron microscopy has provided a powerful tool for this purpose and revealed much concerning the nature of dislocation movement. A cursory literature survey (since this writer cannot profess any competence in the mathematical analysis of dislocations) does not reveal any unit or mechanism which is unaltered by temperature, strain rate, or irradiation.

One prominent feature of strained metal, however, does possess a size of approximately the correct order of magnitude; this is the so-called cell. This cell must not be confused with the "cell" of mosaic structure, produced by heat treatment after small amounts of strain, showing tilt boundaries in an irregular sub-grain boundary network. The cell described here is that discussed extensively by Keh and Weismann (15) in an excellent summary paper and is observed after a considerable amount of strain without subsequent heat treatment. The process by which these cells are formed appears to be the following:

1. At small strain, < 1% straight dislocations are observed.
2. After 1% strain, jogs appear on the dislocations and dislocation interaction can be seen; dislocations cluster inside grains.
3. These clusters join together to form a cell structure whose walls are a tangled network of dislocations, (within the cell, dislocation density is low).
4. As deformation proceeds, the cell walls become more well-defined and align themselves in crystallographic direction.
5. Finally, a regular cell of limiting small size is observed which remains unchanged with increased deformation.

As well as being produced by straining these cells have other interesting properties;

1. The limiting size is a decreasing function of temperature (15) (so far no measurements have been made to indicate whether or not this size is also a function of $\dot{\epsilon}$).
2. Increased impurity content also lowers cell size (16) although limiting (stable) size requires greater strain for achievement (dislocation density, however, increases).
3. Cell size does not however appear to be a function of material grain size.

Obviously, no change in impurity content (inclusions) could be effected by irradiation but some indication exists that dimple geometry is so altered.

If it be argued that d_T is the cell size, then it is necessary to see whether d_T could vary with temperature. (That it may also vary with strain rate or loading speed is ignored for the time being).

Examination of data for steel A212B and A350LF3 show that matching can be accomplished assuming a variable process zone. (Data are matched at equivalent times to reach n and K_{Ic} instead of on a rate basis). If the values obtained are plotted against temperature and the curve extrapolated as a straight line approximation, values of d_T increasing with increased temperature are read giving slightly higher K_{Ic} values.

These considerations at present are largely only speculative. However, both the ligament model proposed by Krafft and the cell model discussed above suggest the physical reality of the postulated process zone.

Development of techniques for transmission electron microscopy of fractured surfaces where a wedging of the irregular surface might occur to provide a sufficiently thin film would be helpful. Examination of these regions might show whether cell structure is produced directly at the fracture surface.

VII. CONCLUSIONS

Fulfillment of general long range objectives - complete understanding of fracture mechanisms - is still a tantalizing chimera; more questions are raised by each increase in the body of knowledge.

However it can be stated that the preliminary general objectives of this research program have been fulfilled.

1. Estimates of K_{Ic} calculated according to the correlation equation

$$K_{Ic} = E\sqrt{2\pi d_T n}$$

can be made on irradiated materials. These values reinforce conclusions drawn from other types of fracture tests that, together with low temperature and high strain rate, irradiation seriously embrittles structural materials.

2. The altered B/r_Y ratio suggests that the size of the plastic zone in irradiated material may no longer be represented by the heretofore used equation. If r_Y, because of an easy glide mechanism, becomes more lobate, the expression defining a rough circle is inadequate.

3. Although correlation of K_{Ic} with the strain hardening exponent is possible, the extremely low values of this number coupled with con-

siderable retained ductility reinforce previous recognition of the fact that strain at maximum load, while an indication of instability, is not an ideal indicator of the fracture event. More appropriately, some value related to total elongation should be chosen. A suitable method of determining this value is still speculative due to the fact that elongation and/or reduction in area are sensitive to specimen geometry.

VIII. ACKNOWLEDGMENTS

It is a pleasure to acknowledge the stimulation and assistance given by the author's colleagues, J. M. Krafft and G. R. Irwin. Further, without the expert and untiring cooperation of F. W. Bird, the difficult and tedious experimental work could not have been carried out. Finally, the fact that the work was done under contract with the U. S. Atomic Energy Commission made it possible.

References

1. G. R. Irwin, "Fracture", Handbook of Physics, Vol. VI, Springer, Berlin, 1958.

2. G. R. Irwin, "Fracture Mechanics", Structural Mechanics", Pergamon Press, 1960.

3. G. R. Irwin, J. A. Kies, and H. L. Smith, "Fracture Strengths Relative to Onset and Arrest of Crack Propagation", Proccedings, ASTM, Vol. 58, p. 640, 1958.

4. A. A. Griffith, "The Theory of Rupture", Proceedings of the International Congress of Applied Mechanics, Delft, p. 55, 1924.

5. J. M. Krafft and A. M. Sullivan, "Effect of Speed and Temperature on Crack Toughness and Yield Strength in Mild Steel", Trans. ASM, 56 (1), p. 160, 1963.

6. J. M. Krafft, "Correlation of Plane Strain Crack Toughness with Strain Hardening Characteristics of a Low, a Medium, and a High Strength Steel", Applied Materials Research, p. 88, April, 1964.

7. L. E. Steele and J. R. Hawthorne, "New Information on Neutron Embrittlement and Embrittlement Relief of Reactor Pressure Vessel Steels", U. S. Naval Research Laboratory 6160, Oct. 6, 1964.

8. J. M. Krafft, F. W. Bird, and J. C. Hahn, Report of NRL Progress, p. 24, Aug. 1962.

9. G. R. Irwin, "Fracture Testing of High Strength Sheet Materials Under Conditions Appropriate for Stress Analysis", NRL Report 5486, July 27, 1960.

10. G. R. Irwin, "Analysis of Stresses and Strains Near the End of a Crack Traversing a Plate", J. Appl. Mech. Vol. 24, p. 361, 1957.

11. ASTM Committee Report: Special Committee on Fracture Testing of High Strength Sheet Materials, ASTM Bulletin 243, p. 29, 1960.

12. J. Eftis and J. M. Krafft, "A Comparison of the Initiation with the Rapid Propagation of a Crack in a Mild Steel Plate", Am. Soc. Mechanical Engrs. Paper 64-Met-16, May, 1964.

13. G. R. Irwin, "Crack Extension Force for a Part-Through Crack in a Plate", Trans. ASME, Vol. 29, E, 4, 1962.

14. A. J. Edwards, "Depth Measurement on Fracture Surfaces", Report of NRL Progress, p. 19, Nov., 1963.

15. A. S. Keh and S. Weismann, "Deformation Substructure in Body-Centered Cubic Metals", Electron Microscopy and the Strength of Crystals, p. 231, Interscience, 1963.

16. P. R. Swann, "Dislocation Arrangements in Face Centered Cubic Metals", Electron Microscopy and the Strength of Crystals, p. 131, Interscience, 1963.

TABLE I

STEEL COMPOSITION

	C	Mn	P	S	Si	Ni	Cr	Mo	V
A350LF3	.14	.52	.031	.032	.25	3.28	.04	.05	.04
A212B	.21	1.08	.010	.026	.27	-	-	-	-

A350LF3 Forging 2.4 in. thick

A212B Plate 4.0 in. thick

TABLE II

	Temperatures in Package		^{o}F	^{o}C
A350LF3	Charpy and Plugs	>	450	232
	Sheet	<	350	177
A212B	Charpy and Plugs	<	350	177
	Sheet	<	350	177

Below 350°F no appreciable effects of annealing have been noted, whereas above 500°F annealing effects (if present) would tend to improve fracture properties.

TABLE III

	ΔT at C_V 20 ft-lb		ΔK_{Ic}	$\Delta \sigma_{YS}$
	^{o}F	^{o}C	Ksi $\sqrt{in.}$	Ksi
A350LFB	+ 615	+ 323	- 32	+ 33
A212B	+ 390	+ 199	- 34	+ 36

TABLE IV

	Control		Irradiated	
	in. x 10^{-6}	Microns	in. x 10^{-6}	Microns
A350LF3	70.0	1.78	1590.0	40.38
A212B	28.9	.73	254.4	6.46

TABLE V

Sheet	B/r_Y Control	Irradiated
A350LF3	10	30
A212B	10	30

where B = 0.10 in.

Charpy at C_V 30 ft-lbs

A350LF3	3.3	40*
A212B	3.6	40

where B = .394 in.

*proportionate, since no C_V 30 value

and

$$r_Y = \frac{1}{2\pi}\left(\frac{K_{Ic}}{\sigma_{YS}}\right)^2$$

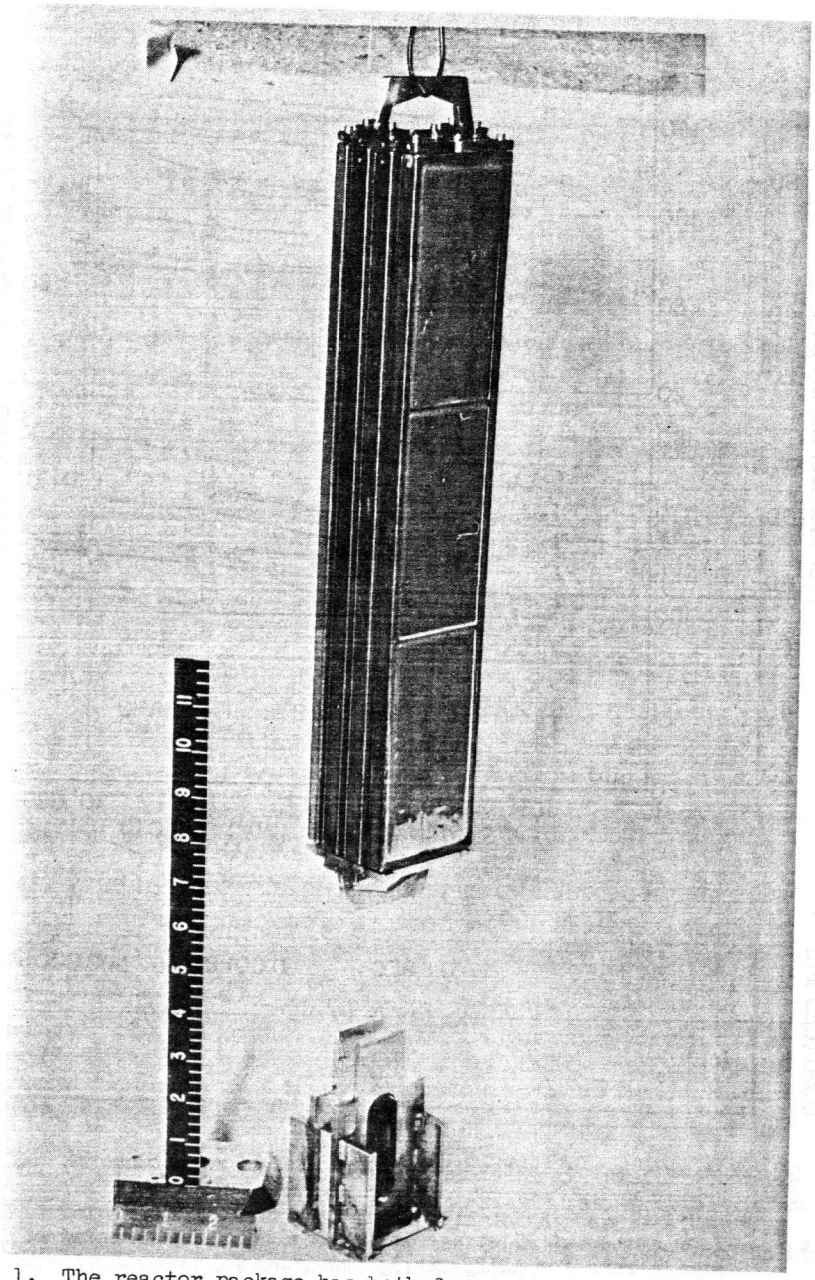

Fig. 1. The reactor package has both frame and skin made of stainless steel. Flushed with helium and pressurized for leak detection, it is finally closed by welding.

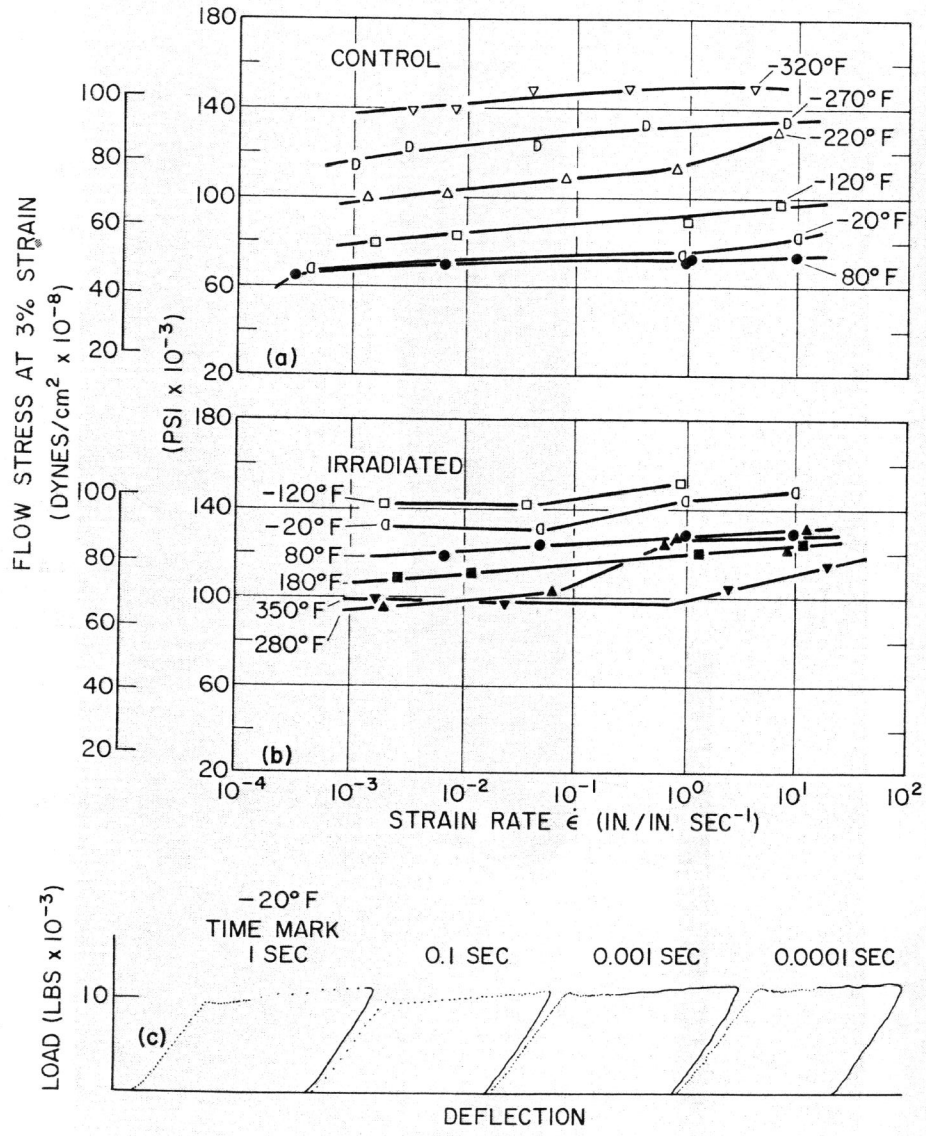

Fig. 2. Flow stress at 3% strain is shown plotted against log of strain rate for A212B steel: as received (a); irradiated (b). Examples of load deformation records are given for the irradiated material, (c).

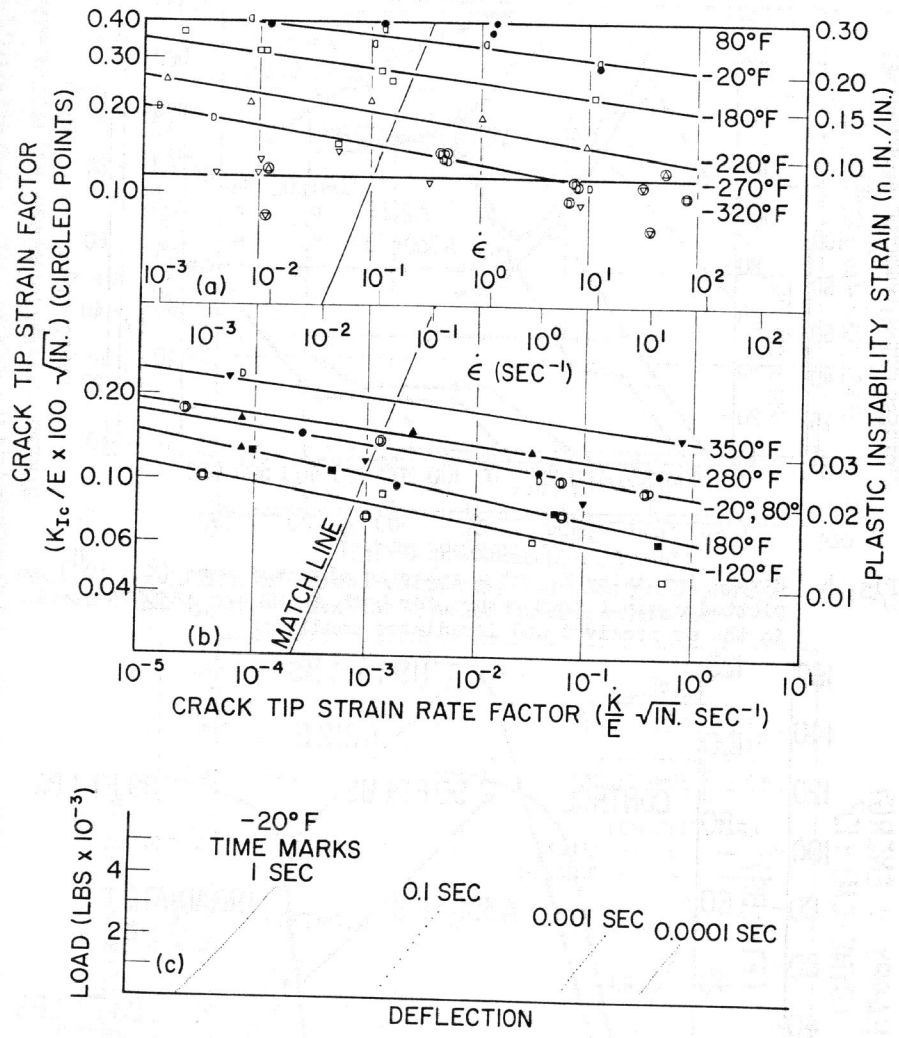

Fig. 3. Stress intensity K_{Ic} is plotted against crack tip stress rate factor for A212B steel; a scale for the values of the strain-hardening exponent n is also included: as received (a); irradiated (b). Examples of the tensile fracture records are given for the irradiated material (c).

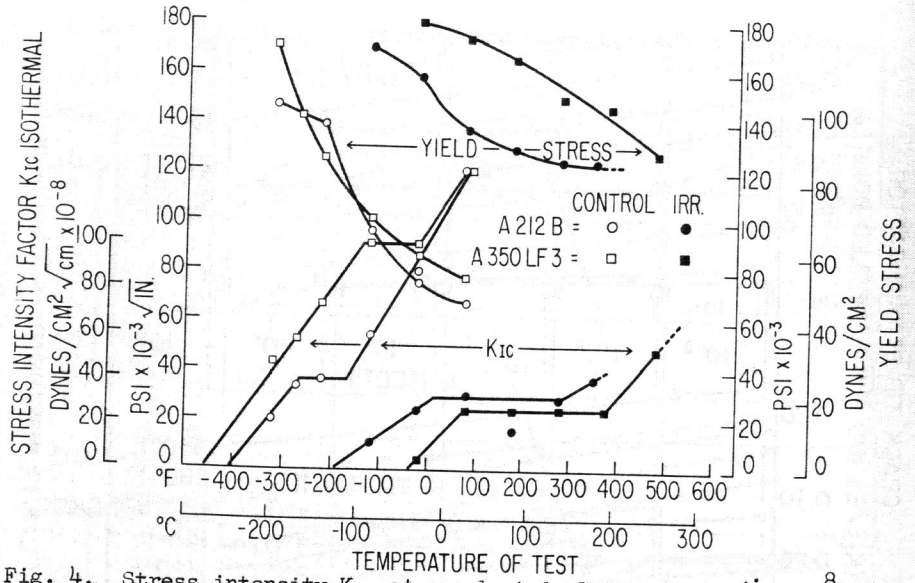

Fig. 4. Stress intensity K_{Ic} at a selected elevated rate ($\dot{K} = 10^8$) is plotted against temperature for both A212B and A350LF3 steels in the as received and irradiated condition.

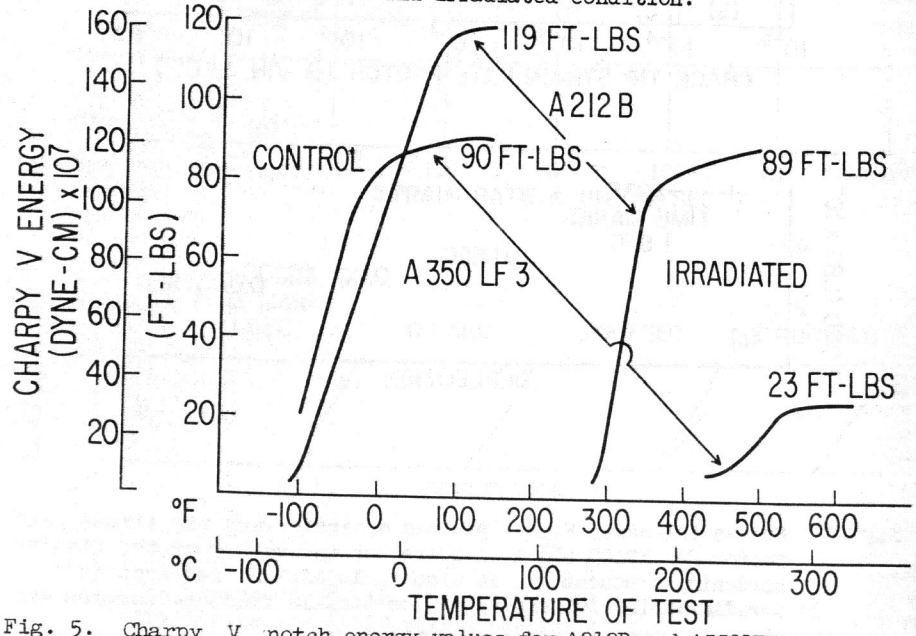

Fig. 5. Charpy V notch energy values for A212B and A350LF3 steels are compared in the as received and irradiated condition. For estimative purposes, C_V 30 ft-lbs is taken to represent the nil ductility temperature (NDT).

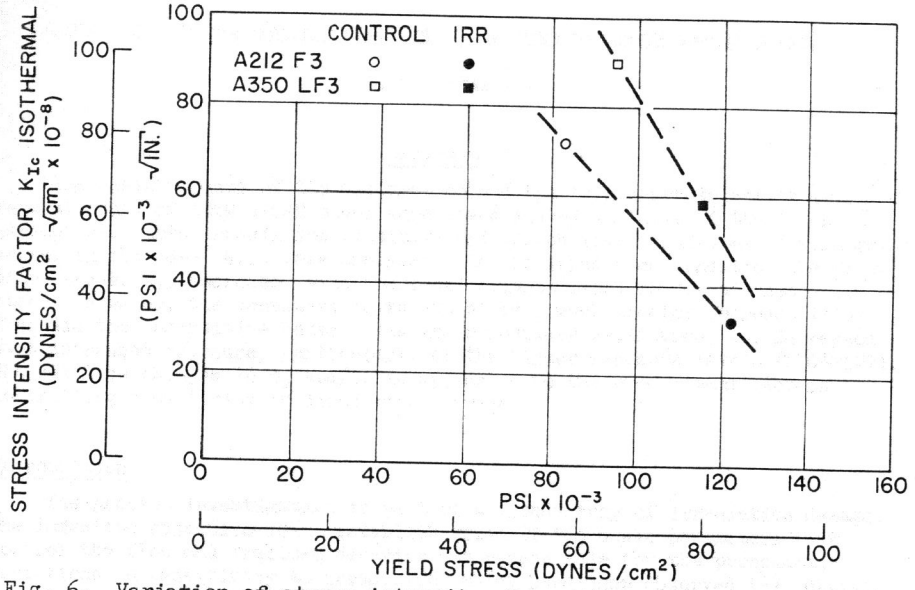

Fig. 6. Variation of stress intensity, K_{Ic} with yield stress; both K_{Ic} and σ_{YS} at equivalent dynamic loading condition.

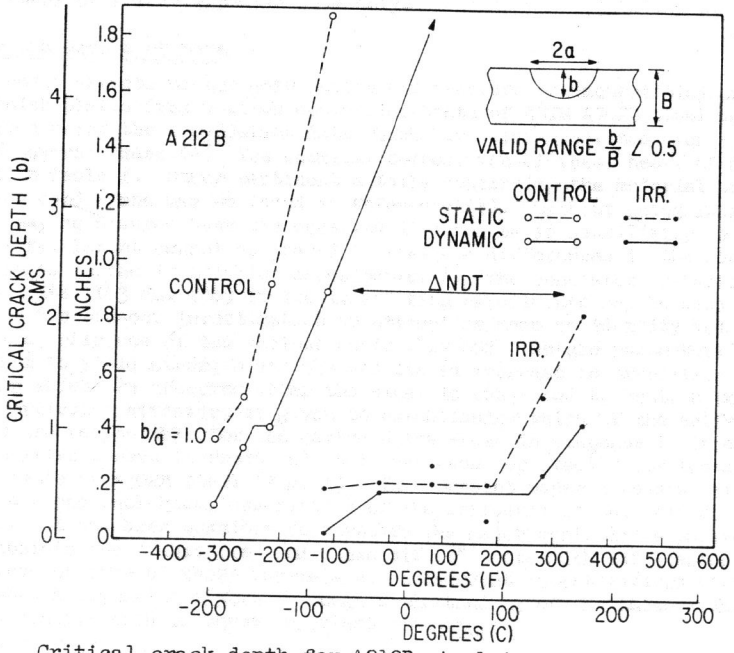

Fig. 7. Critical crack depth for A212B steel is compared for static and dynamic load conditions.